# Autoignition of isooctane beyond RON and MON conditions

2018-01-1254

# Autoignition of isooctane beyond RON and MON conditions

**J. Masurier, M. U. Waqas, S. M. Sarathy, B. Johansson**
King Abdullah University of Science and Technology,
Clean Combustion Research Center,
23955-6900, Thuwal, Saudi Arabia

## Abstract

The present study experimentally examines the low temperature autoignition area of isooctane within the in-cylinder pressure – in-cylinder temperature map.

Experiments were run with the help of a CFR engine. The boundaries of this engine were extended so that experiments could be performed outside the domain delimited by RON and MON traces. Since HCCI combustion is governed by kinetics, the rotation speed for all the experiments was set at 600 rpm to allow time for low temperature heat release (LTHR). All the other parameters (intake pressure, intake temperature, compression ratio and equivalence ratio), were scanned, such as the occurrence of isooctane combustion.

The principal results showed that LTHR for isooctane occurs effortlessly under high intake pressure (1.3 bar) and low intake temperature (25 °C). Increasing the intake temperature leads to the loss of the LTHR, and therefore to a smaller domain on the pressure-temperature trace. In such a case, the LTHR domain is restricted from 20 to 50 bar in pressure and from 600 to 850 K in temperature. By slightly decreasing the intake pressure, the LTHR domain remains unchanged, but the LTHR tends to disappear, and finally, at 1.0 bar, the LTHR domain ceases to exist. When the equivalence ratio is moved from 0.3 to 0.4, the LTHR domain is delimited in the same range of pressure and temperature, but the start of combustion occurs slightly earlier for the same pressure-temperature trace. Similar conclusions were drawn regarding the variation of both intake pressure and temperature, except that few LTHR points were observed under 1.0 bar intake.

## Introduction

To reduce $CO_2$ and pollutant emissions and increase efficiency, development of internal combustion engines has been pushed towards advanced combustion engines, also called low temperature combustion engines [1], [2]. These engines offer promising results, but their universal implementation depends on several factors, making it necessary to find a fuel which perfectly matches engine requirements [3]. As a result, only a few candidates can substitute for gasoline and diesel [4].

Fuels for spark ignition (SI) engines are selected according to their tendency to knock, which corresponds to the autoignition of the end gases within the combustion chamber [5]; a thorough understanding of the fuel behavior on a wide operating range of the engine is therefore mandatory. Research octane number (RON) [6] and motor octane number (MON) [7] are the two main properties which reflect fuel behavior. Together, these two octane numbers delimit the operating range of fuels in engines, but future engines will tend to operate beyond these boundaries, making RON and MON obsolete [8]. To address that issue, Kalghatgi [9] introduced the octane index OI = RON – KS, in which S is fuel sensitivity (S = RON-MON), and K is a parameter function of the operating condition. The OI helps to compare two fuels and indicates whether fuels with the same OI and pressure-temperature trace history will behave the same, regardless of fuel composition [10]. OI also shows that current and future SI engines require fuel with high RON and high S. Similar conclusions have been reached by other researchers [11]–[13], but they also show that the use of the OI is limited to describing the entire behavior of the combustion. Some works suggest that additional metrics, similar to RON, MON or OI, are required for describing fuel behavior [13], [14]; but physical properties such as ignition delay times [15], [16], density, atomic weight, lower heating value [17], flame speed, viscosity and volatility, must also be considered.

With the goal of investigating their autoignition and combustion processes, fuels were studied with the help of homogeneous charge compression ignition (HCCI) experiments, because of their ability to use a wide variety of fuels [18]. The results emphasized the significance of low temperature heat release (LTHR) on combustion behavior [13], [19]. In particular, Sjoberg *et al*. [20] pointed out that the presence of LTHR makes combustion control difficult under a wide operating range. A representation of the start of combustion in a temperature-pressure map was initiated by Truedsson *et al*. [21], [22] and revealed that some fuels react with or without LTHR, depending on the operating conditions. Similar results were observed by Contino *et al.* [23], but with a different representation. They proposed to describe the combustion process by mapping the CA50 as a function of pressure and temperature conditions at 25 crank angles before top dead center, and by using a linear regression on the same parameters. To this end, they emphasized the LTHR. Finally, recent studies, conducted by Szybist *et al.* [12] and Splitter *et al*. [24], proposed to combine an estimation of the pressure-temperature history of the end gases with ignition delays computed on the same map to evaluate fuel behavior and the presence of LTHR.

All these works suggest that operating conditions which lead to the pressure-temperature history within the combustion chamber of an engine are significant for investigating the fuel behavior. However, the full description cannot be limited to a single metric. A good way to provide understanding of fuel behavior is to map the autoignition of practical fuels within a pressure-temperature map. Moreover, because of the difficulty in assessing data from the end-gases, HCCI experiments should be performed. The present study aims to

experimentally investigate the combustion behavior of isooctane under a wide range of HCCI operating conditions. The study will focus especially on autoignition and the LTHR domain within a pressure-temperature map.

## Experimental setup

A single cylinder Cooperative Fuels Research (CFR) engine was used to perform the present experiments. Figure 1 shows a scheme of the CFR engine and Table 1 provides its main features. The experimental setup was modified to run experiments at very lean conditions. The intake pipe includes two heaters which allow preheating of the air. The first heater warms the air flow while the second heater, which surrounds the intake pipe, maintains a constant temperature all along the intake pipe. Air flow is controlled through a mass flow controller which enables constant intake pressure regulation. In addition, the mass flow controller provides a measurement of the flow admitted under standard conditions. Finally, the fuel is injected through a gasoline port fuel injector located close to the intake valve. The amount of fuel injected is controlled by managing the injection timing. A liquid flowmeter, mounted on the fuel line and coupled with the air mass flow controller, enables monitoring of the equivalence ratio.

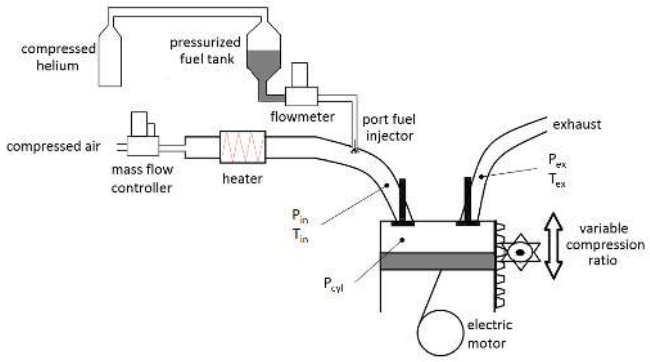


*Figure 1: Schematic of experimental setup*

In-cylinder pressure, intake pressure and exhaust pressure were measured using AVL pressure transducers. Acquisition was carried out with a resolution of 0.2 crank angle, using an AVL encoder. Two thermocouples (one in the intake port, one in the exhaust port), were used to compute initial conditions at the intake valve closure. Finally, results were recorded for 200 consecutive cycles, and a typical thermodynamic analysis [25], based on the average of the same 200 cycles, was performed.

## Results and discussion

The aim of the present study was to experimentally investigate the low temperature heat release of isooctane within the in-cylinder pressure – in-cylinder temperature map. All experiments were performed for a rotation speed of 600 rpm. Because HCCI combustion is dominated by kinetics reactions which are time-related, a low rotation speed allowed more time for low temperature reactions to appear [20], [26].

*Table 1: Main properties of CFR engine.*

| Parameter | Unit | Value |
|---|---|---|
| Displaced volume | cc | 611.7 |
| Stroke | mm | 114.3 |
| Bore | mm | 82.55 |
| Connecting rod | mm | 256 |
| Compression ratio | - | 4:1 to 19:0 |
| Number of valves | - | 2 |
| Exhaust valve opening | CA ATDC | 140 |
| Exhaust valve closure | CA ATDC | -345 |
| Inlet valve opening | CA ATDC | -350 |
| Inlet valve closure | CA ATDC | -146 |

### *Boundaries of the CFR engine*

Before investigating the low temperature heat release of isooctane, the boundaries of the CFR engine were examined, as well as the potential of this experimental setup for studying the low temperature domain of isooctane.

The CFR engine is probably the best tool for experimentally investigating the behavior of fuels within the in-cylinder pressure – in-cylinder temperature map, because of its variable compression ratio. Here, the compression ratio ranges from 4 to 19. The experimental setup also permits adjustment of both the intake temperature, from ambient temperature (~25 °C) to 150 °C, and the intake pressure, from 0.5 bar to 1.3 bar, which together extend the usual limits of the CFR. Figure 2 shows experimental motoring traces of the compression stroke, from the intake valve closing to the peak pressure, at 600 rpm into the in-cylinder pressure – in-cylinder temperature map for both minimum and maximum conditions of compression ratio, of intake temperature and pressure.

Figure 2 shows that the compression ratio slightly modifies pressure-temperature traces for the same initial conditions, instead of overlapping. This difference is due to the presence of hot gases from the previous cycle, whose amount is inversely proportional to the compression ratio. Moreover, as expected, the upper limit was reached for the minimum intake temperature and the maximum intake pressure, while the lower limit was reached with the maximum intake temperature and minimum intake pressure. These two lines delimit the current boundaries of the CFR engine and provide the potential for investigating low temperature conditions of fuels, especially if the ignition delays of the fuel are known.

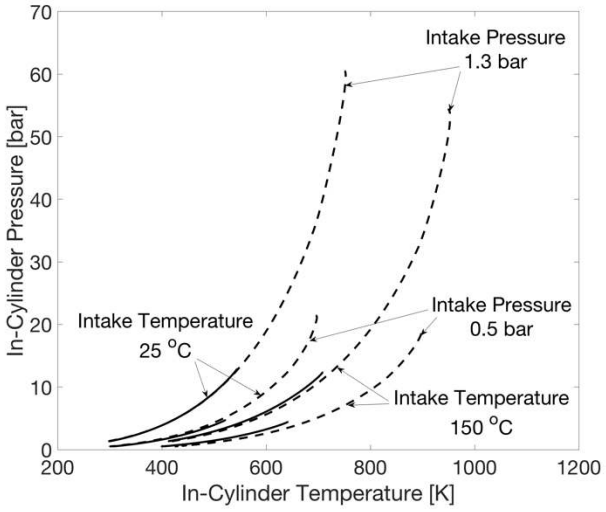


*Figure 2: In-cylinder pressure vs. in-cylinder temperature traces for compression stroke of motoring cases at 600 rpm. Solid lines correspond to minimum compression ratio. Dashed lines correspond to maximum compression ratio.*

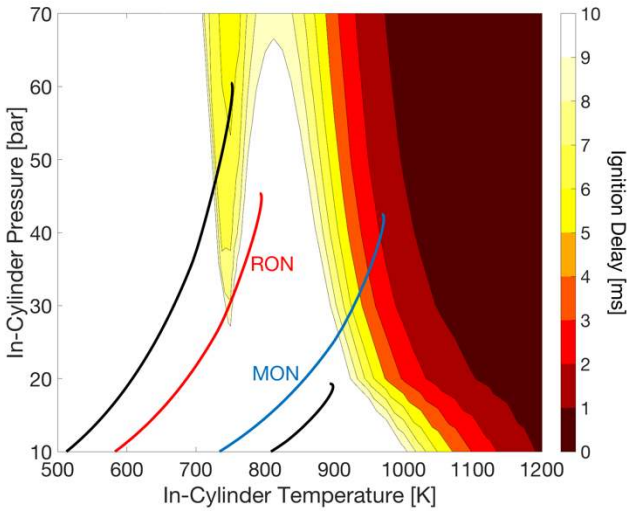


*Figure 3: Ignition delays of isooctane for equivalence ratio of 0.3 within in-cylinder pressure vs. in-cylinder temperature map. Black lines correspond to upper and lower limits of CFR engine. Red and blue lines correspond to in-cylinder pressure – in-cylinder temperature trace of RON and MON, respectively.*

To assess its ignition delays as a function of conditions of pressure and temperature, many studies were conducted on isooctane as fuel. In the present study, the kinetics scheme proposed by Atef *et al.* [27] was used to find ignition delays of isooctane under typical HCCI conditions. The mechanism involves 2768 species and consists of 9220 reactions. The first ignition delays of isooctane for an equivalence ratio of 0.3 are shown in Figure 3. Upper and lower limits of the CFR are plotted, as well as pressure-temperature traces of both RON and MON, respectively defined by ASTM 2799 [6] and ASTM 2800 [7]. Results show that the CFR engine enables investigation of fuel behavior beyond the domain restricted by RON and MON. Furthermore, by extending the operating domain of the CFR engine, it should be possible to observe the low temperature ignition of isooctane.

## *Low temperature and high temperature ignitions*

In the present study, both low and high temperature autoignition points are defined as the crank angles where low temperature combustion and main combustion initiate; therefore, they respectively represent low temperature and high temperature ignition delays. Figure 4 shows a graphic definition of both low temperature and high temperature autoignition points. The low temperature autoignition point is identified as the crank angle, where the rate of heat release reaches a threshold value of 0.2 J/CA, as in [21], [22]. This point is considered only if it can be clearly observed. To identify the main temperature autoignition, it was decided to fit the main combustion peak by a normal distribution; the autoignition point corresponds to the crank angle where the fit also reaches a threshold of 0.2 J/CA. The gap between these two points finally delimits the domain of both the low temperature heat release and the negative temperature coefficient. From these two crank angles, the corresponding in-cylinder pressure and in-cylinder temperature were then extracted to assess the low temperature domain within the in-cylinder pressure – in-cylinder temperature map.

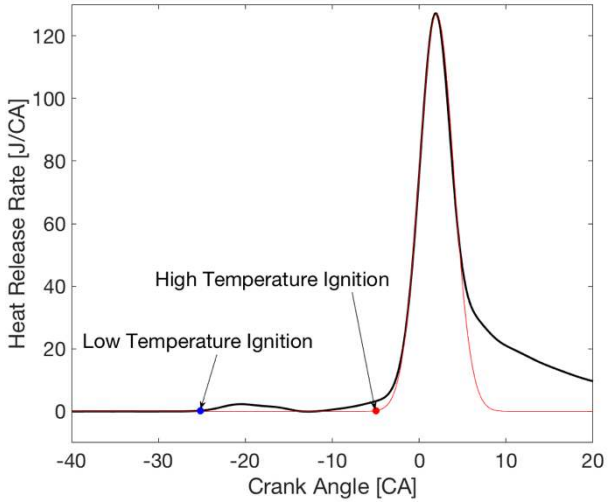


*Figure 4: Definition of low and high temperature autoignition points. Heat release rate corresponds to the average over 200 cycles. Red peak corresponds to normal distribution fitting the main combustion peak.*

## *Experimental matrix*

All the experiments were conducted at 600 rpm; and the study focused on 0.3 and 0.4 equivalence ratios. To evaluate low temperature domain within the in-cylinder pressure – in-cylinder temperature map for a single equivalence ratio, the three main variables, intake temperature, intake pressure and compression ratio, were varied, so that isooctane exhibited combustion from misfiring to combustion where the CA50 (the crank angle for 50% of the fuel burnt), is located close to the top dead center (TDC). The intake temperature was increased from the ambient temperature (~25 °C) to a maximum temperature of 150 by a step of 25 °C. Intake pressure was first set at maximum pressure permitted by the experimental setup (1.3 bar), and the compression ratio was adjusted to observe isooctane combustion from misfiring to

a combustion located close to the TDC. The experiments were then repeated by decreasing the intake pressure until the compression ratio was at its top value and isooctane combustion did not occur. As a result, the intake pressure was used from 1.0 bar to 1.3 bar.

### *Effect of the compression ratio*

Previous results for motoring traces showed that the compression ratio slightly modified the in-cylinder pressure - in-cylinder temperature trace when varied from minimum to maximum. In firing cases, with isooctane as fuel, the compression ratio varies less to achieve combustion from misfiring to a combustion phased close to the TDC. For instance, for intake conditions set at 1.3 bar and 25 °C, the compression ratio is increased from 15.6 to 16.7. The in-cylinder pressure – in-cylinder temperature traces for these conditions are plotted in Figure 5.

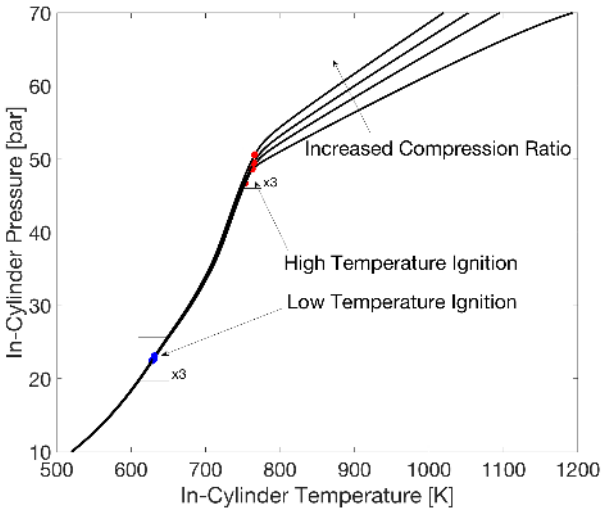


*Figure 4: In-cylinder pressure – in-cylinder temperature traces for different compression ratios at 1.3 bar and 25 °C. Boxes correspond to the uncertainties of both low and high temperature ignition points multiplied by 3.*

The results in Figure 5 show that all the traces form a single trace before the first ignition, meaning that the compression ratio does not impact the pressure temperature trace as long as the intake conditions remain constant. For fuels exhibiting a definite low temperature heat release, compression ratio can influence combustion phasing of the low temperature heat release. Therefore, the pressure – temperature trace can be expected to be influenced after the first ignition. In the case of isooctane, the low temperature heat release is very small (Figure 5). As a result, the pressure – temperature trace between the two ignition points remains nearly unchanged. Finally, in the main combustion, a clear divergence occurs because increasing the compression ratio allows it to reach a higher maximum pressure at the end of the compression stroke. This result was expected, as the CA50 varies from a late combustion to a combustion phased around the TDC.

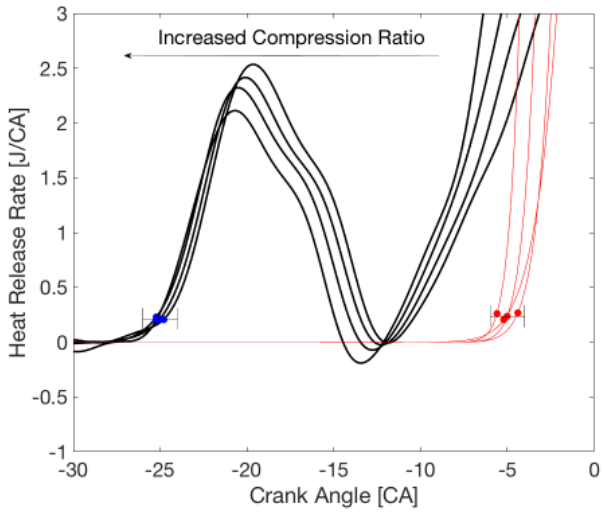


*Figure 5: Enlarged view of heat release ratio at 1.3 bar and 25 °C for different compression ratios. Blue and red points respectively correspond to low and high temperature ignition. Error bars correspond to standard deviation of a single low and high temperature ignition point.*

Finally, regarding the two ignition points in Figure 5, all the low temperature ignition points collapse and do not appear to be influenced by the compression ratio, while the high temperature ignition point is almost always located at the inflexion point of the pressure – temperature trace and is influenced by the compression ratio. Actually, the high temperature ignition point is obtained through a fitting of the main combustion peak, which depends greatly on the compression ratio.

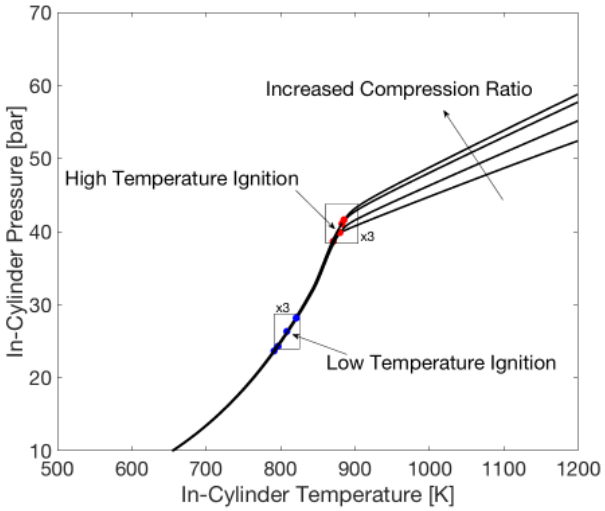


*Figure 6: In-cylinder pressure – in-cylinder temperature traces for different compression ratios at 1.3 bar and 125 °C. Boxes correspond to the uncertainties of both low and high temperature ignition points multiplied by 3.*

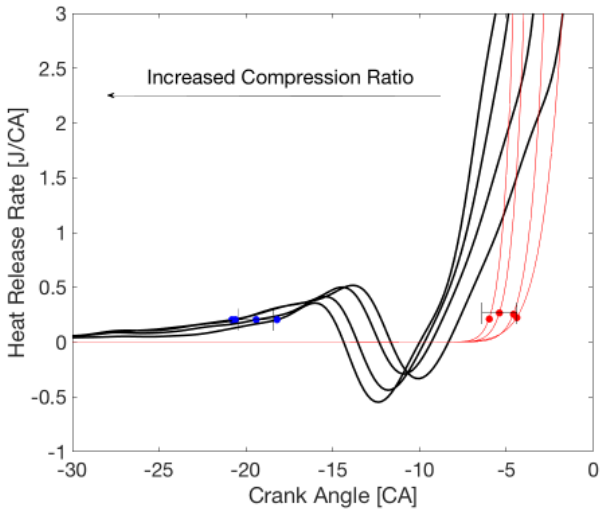


*Figure 7: Enlarged view of the rate of heat release at 1.3 bar and 125 °C for different compression ratio. Blue and red points respectively correspond to the low temperature ignition and high temperature ignition. Error bars correspond to the standard deviation of a single low and high temperature ignition point.*

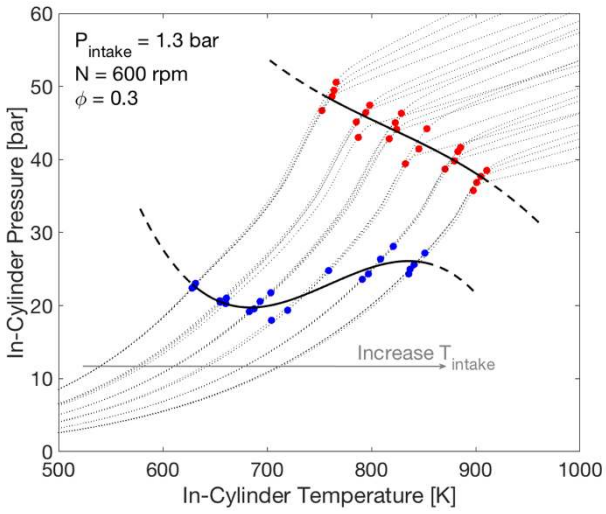


*Figure 8: In-cylinder pressure - in-cylinder temperature traces for intake pressure at 1.3 bar, equivalence ratio 0.3 and intake temperature range from 25 to 150 °C. Blue and red symbols respectively correspond to low and high temperature ignition. Solid lines are the interpolation of ignition points. Dashed lines are extrapolation.*

Regarding the results in Figures 7 and 8, obtained for a different case (1.3 bar and 125 °C), the same conclusions can be drawn even if the compression ratio used was different (from 14.5 to 15.7). However, the low temperature ignition point does not collapse on the pressure – temperature trace. For this case of higher intake temperature, the low temperature heat release exhibits a lower peak as the amount of fuel within the combustion chamber is less for maintaining the equivalence ratio (Figure 8). Moreover, as the increase in heat release is slow, compared to the case at 25 °C, the tracking of the low temperature ignition point is less easy and this phasing can occur in a variable range of crank angle, which has an impact when it is displayed in Figure 7.

## *Low temperature domain of isooctane*

### Results at equivalence ratio 0.3

In the present study, the low temperature domain of isooctane is identified as the area between the low temperature ignition and the high temperature ignition points. For a clear analysis of this domain within the in-cylinder pressure – in-cylinder temperature map, the pressure-temperature traces obtained for the different intake pressure tested were plotted. The results are shown with respect to the intake pressure in Figures 9 through 12. The low temperature ignition points are displayed on these different graphs only if the low temperature heat release is clearly observed. For intake pressure at 1.3 bar and 1.2 bar, the low temperature heat releases were well identified for the intake temperature used. For 1.1 bar, the low temperature heat releases were only observed to an intake temperature of 75 °C and not above. Finally, for intake pressure of 1.0 bar, it was not possible to obtain pressure-temperature traces before 75 °C, as for that temperature and pressure, the compression ratio was already set to its maximum limit. Moreover, the results do not show any low temperature heat release in this case, explaining the low temperature ignition points missing in Figure 12.

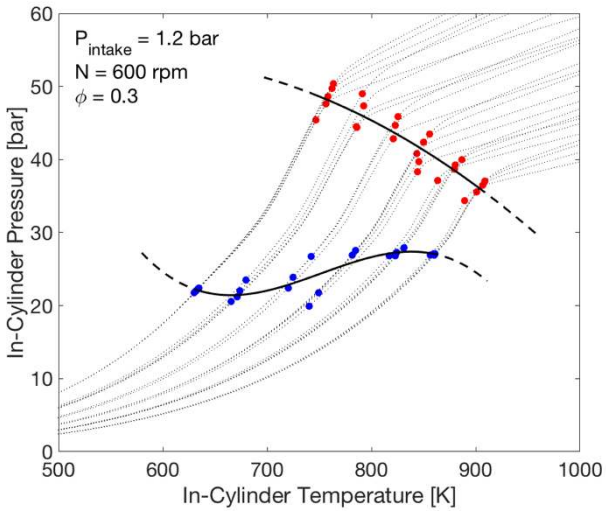


*Figure 9: In-cylinder pressure - in-cylinder temperature traces for intake pressure at 1.2 bar, equivalence ratio 0.3 and intake temperature range from 25 to 150 °C. Blue and red symbols respectively correspond to the low and the high temperature ignition. Solid lines are interpolation of ignition points. Dashed lines are extrapolation.*

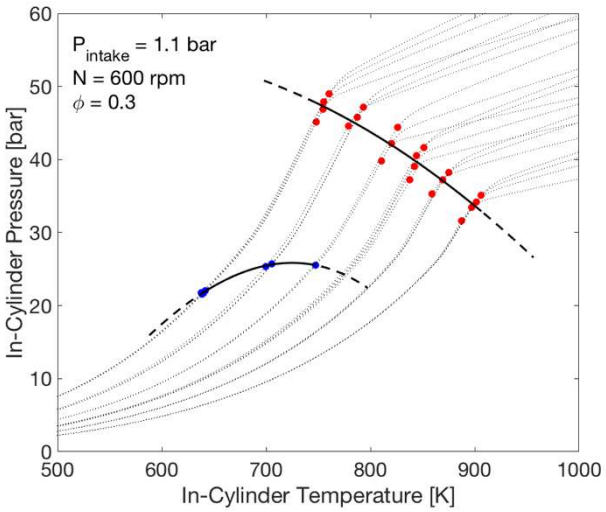


*Figure 10. In-cylinder pressure - in-cylinder temperature traces for intake pressure at 1.1 bar, equivalence ratio 0.3 and intake temperature range from 25 to 150 °C. Blue and red symbols respectively correspond to low and high temperature ignition. Solid lines are the interpolation of ignition points. Dashed lines are extrapolation.*

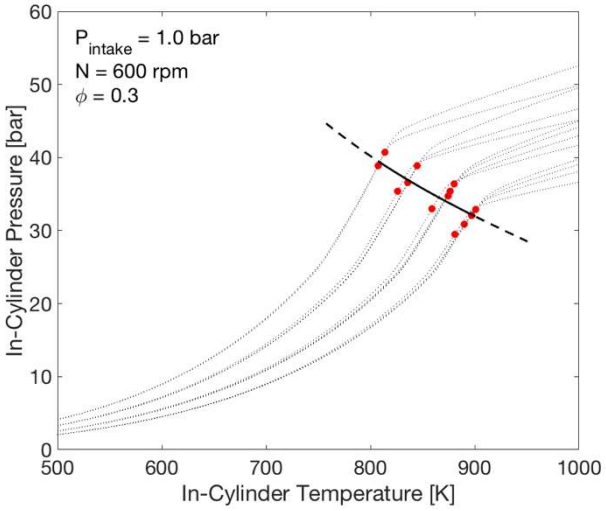


*Figure 11. In-cylinder pressure - in-cylinder temperature traces for intake pressure at 1.3 bar, equivalence ratio 0.3 and intake temperature range from 75 to 150 °C. Red symbols respectively correspond to the low temperature ignition and the high temperature ignition. Solid line is the interpolation of the high temperature ignition points. Dashed line is extrapolation.*

In Figure 9, the effect of intake temperature can be observed on both low and high temperature ignition points. The high temperature ignition points show a kind of linear decrease in the in-cylinder pressure – in-cylinder temperature map, meaning that the main combustion can begin earlier by increasing the intake temperature, which is the expected effect. For low temperature ignition, the solid line shows that--with respect to the intake temperature--the low temperature domain narrows. Moreover, this type of shape could give rise to consideration of the ignition delay curve observed for fuel which exhibits low temperature combustion and negative temperature coefficient. Therefore, if it were possible to get data at a higher intake temperature, the two solid lines could be expected to merge. Similar conclusions could be reached at 1.2 bar (Figure 10), but at a lower intake pressure the low temperature heat release does not appear, therefore, no conclusion can be drawn from these cases.

Finally, these different areas are compared in Figure 13 and a conclusion regarding the effect of the intake pressure can be achieved. The ignition points at high temperatures showed parallel trends and it can be concluded that the intake pressure expands the low temperature area, but it was previously shown that the points used to define the high temperature ignition changed with respect to the compression ratio. As a result, all these trends can be merged into a single curve, representing the upper limit of the low temperature area. Regarding the low temperature ignition curves, it can be concluded that the intake pressure enables the low temperature area to expand. Finally, all these results show that the low temperature area can be experimentally identified within the in-cylinder pressure – in-cylinder temperature map.

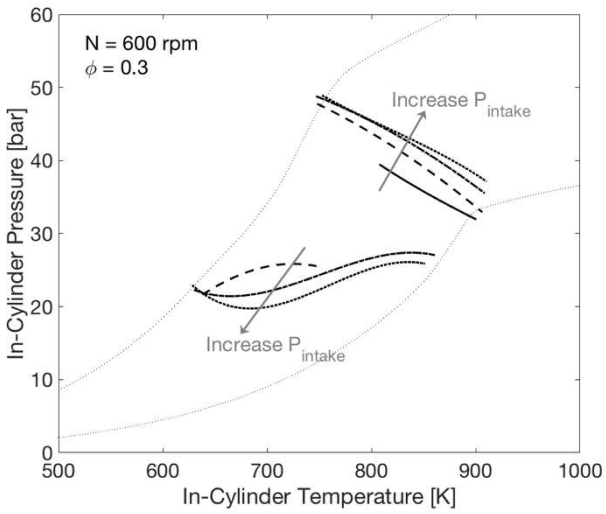


*Figure 12: Effect of intake pressure on low temperature domain within the in-cylinder pressure - in-cylinder temperature map at equivalence ratio 0.3.*

**Results at equivalence ratio 0.4**

Figures 14 to 17 show low temperature areas within the in-cylinder pressure – in-cylinder temperature map for different intake pressures at equivalence ratio 0.4. Globally, the results for the different intake pressures are similar to those obtained at equivalence ratio 0.3, but low temperature ignitions were better observed for 1.1 and 1.0 as intake pressures, even if the low temperature ignition is only visible for the intake temperature at 25 °C and 1.0 bar.

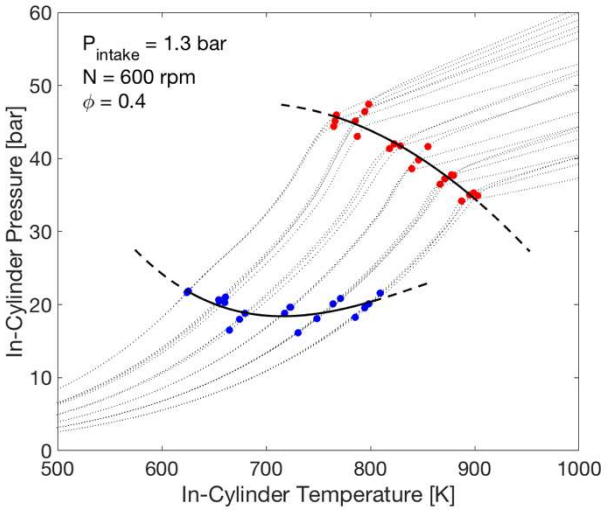


*Figure 13: In-cylinder pressure - in-cylinder temperature traces for intake pressure at 1.3 bar, equivalence ratio 0.4 and intake temperature range from 25 to 150 °C. Blue and red symbols respectively correspond to low and high temperature ignition. Solid lines are interpolation of ignition points. Dashed lines are extrapolation.*

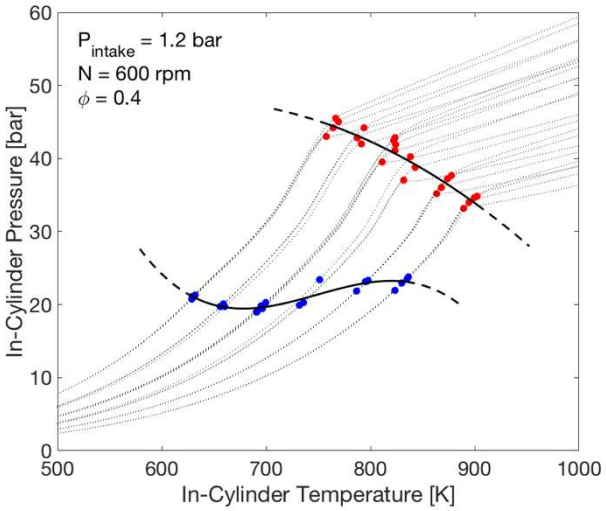


*Figure 14: In-cylinder pressure - in-cylinder temperature traces for intake pressure at 1.2 bar, equivalence ratio 0.4 and intake temperature range from 25 to 150 °C. Blue and red symbols respectively correspond to low and high temperature ignition. Solid lines are interpolation of ignition points. Dashed lines are extrapolation.*

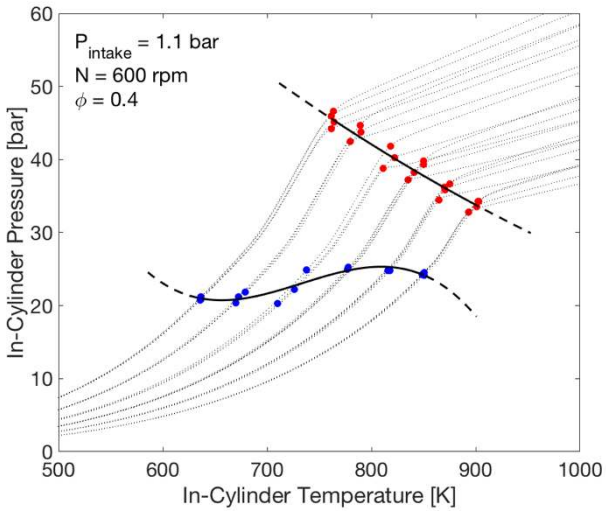


*Figure 15: In-cylinder pressure - in-cylinder temperature traces for intake pressure at 1.1 bar, equivalence ratio 0.4 and intake temperature range from 25 to 150 °C. Blue and red symbols respectively correspond to low and high temperature ignition. Solid lines are interpolation of ignition points. Dashed lines are extrapolation.*

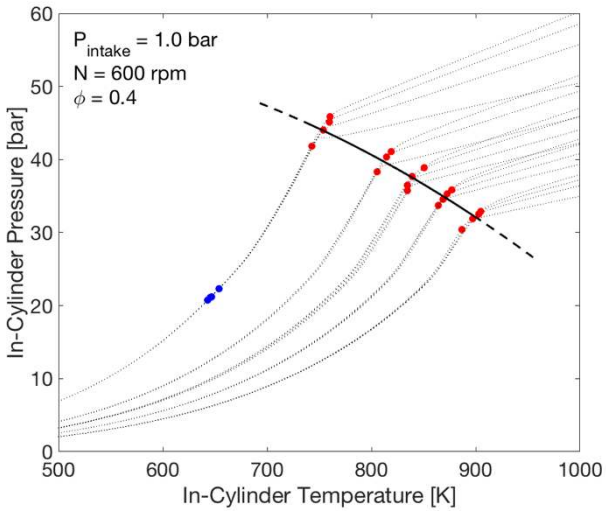


*Figure 16: In-cylinder pressure - in-cylinder temperature traces for intake pressure at 1.0 bar, equivalence ratio 0.4 and intake temperature range from 25 to 150 °C. Blue and red symbols respectively correspond to low and high temperature ignition. Solid line is interpolation of high temperature ignition points. Dashed line is extrapolation.*

Figure 18 combines all the trends obtained at equivalence ratio 0.4. Similar to Figure 13 for equivalence ratio 0.3, the increase in intake

pressure expanded the low temperature area, making the low temperature ignition more sensitive when the engine is supercharged.

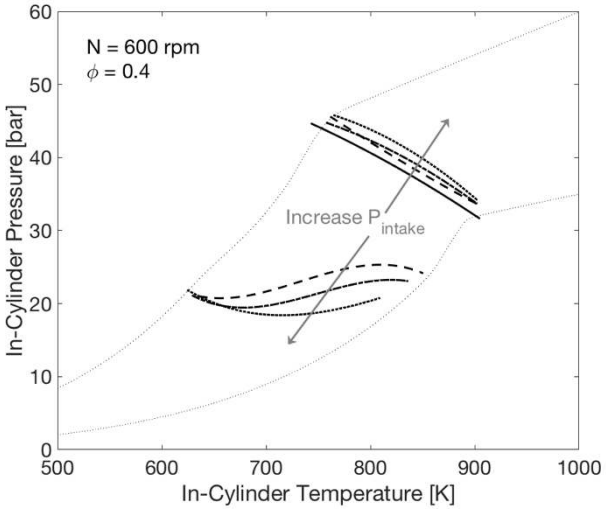


*Figure 17: Effect of intake pressure on low temperature domain within the in-cylinder pressure - in-cylinder temperature map at equivalence ratio 0.3.*

Finally, results between the two equivalence ratios investigated can be compared. At first glance, they appear to be alike, but by including the results within the same plot (Figure 19), the high temperature ignition is seen to be identical, but the low temperature area is somewhat wider at equivalence ratio 0.4. Actually, increasing the equivalence ratio enables the fuels to more easily exhibit low temperature heat release. Therefore, a wider domain of low temperature area is expected with the in-cylinder pressure – in-cylinder temperature map at such an equivalence ratio.

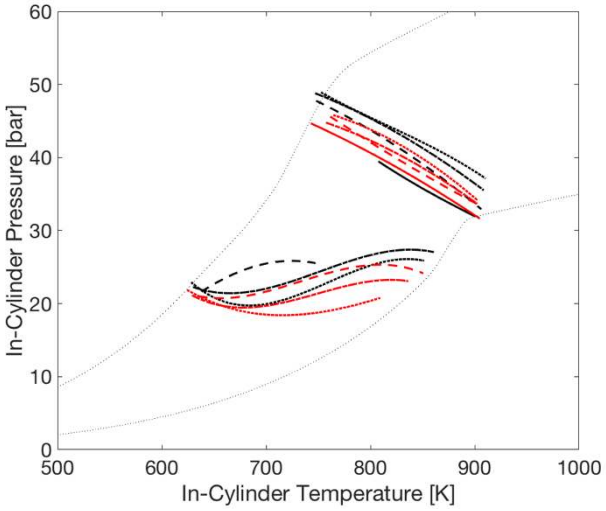


*Figure 18: Low temperature domains within the in-cylinder pressure - in-cylinder temperature map at equivalence ratio 0.3 (black lines) and 0.4 (red lines).*

## Summary and Conclusions

The low temperature autoignition for isooctane as fuel has been experimentally investigated under lean conditions in the in-cylinder pressure – in-cylinder temperature map. A modified CFR engine was used. This model permits the study of fuel behavior outside of the restricted area delimited by RON and MON. The investigation was performed at 600 rpm for various intake pressures, intake temperatures, compression ratios and two equivalence ratios. The following conclusions can be drawn:

- High temperature ignition occurs close to the inflexion point in the in-cylinder pressure – in-cylinder temperature map. Its location is sensitive to CA50, and therefore sensitive to the compression ratio.
- Low temperature ignition is stable when low temperature heat release is clearly observed, but when its intensity decreases, its location becomes sensitive.
- In the pressure – temperature map, the high temperature ignition decreases almost linearly with respect to the intake temperature, and the low temperature domain becomes smaller.
- The intake pressure clearly shows that a supercharged engine leads to the occurrence of low temperature heat release as the low temperature area becomes wider with that parameter. However, only the beginning of the combustion is affected; the location of the main combustion will remain the same.
- Finally, the equivalence ratio also expands the area of the low temperature heat release.

Future research will focus on greater expansion of the domain currently covered by the CFR engine. One of the challenges will be to achieve data at higher temperatures in order to merge the trend of low temperature ignition with high temperature ignition. However, experiments at higher intake pressure and lower intake temperature could help to determine whether the low temperature ignition trend will follow the same tendency that the ignition delay provides through fuel oxidation. Finally, as the assessment of the low temperature area seems sensitive to the compression ratio, and therefore the CA50, all traces should focus on a single CA50.

## References

[1] X. Lu, D. Han, and Z. Huang, "Fuel design and management for the control of advanced compression-ignition combustion modes," *Prog. Energy Combust. Sci.*, vol. 37, no. 6, pp. 741–783, 2011.

[2] A. K. Agarwal, A. P. Singh, and R. K. Maurya, "Evolution, challenges and path forward for low temperature combustion engines," *Prog. Energy Combust. Sci.*, vol. 61, pp. 1–56, 2017.

[3] G. T. Kalghatgi, *Fuel/Engine Interactions*. 2014.

[4] C. Bae and J. Kim, "Alternative fuels for internal combustion engines," *Proc. Combust. Inst.*, vol. 36, pp. 3389–3413, 2017.

[5] Z. Wang, H. Liu, and R. D. Reitz, "Knocking combustion in spark-ignition engines," *Prog. Energy Combust. Sci.*, vol. 61, pp. 78–112, 2017.

[6] ASTM International, “Standard Test Method for Research Octane Number of Spark-Ignition Engine Fuel - D2699 - 08,” *ASTM Int.*

[7] ASTM International, “Standard Test Method for Motor Octane Number of Spark-Ignition Engine Fuel - D2700 - 08,” *ASTM Int.*

[8] G. T. Kalghatgi, “Developments in internal combustion engines and implications for combustion science and future transport fuels,” *Proc. Combust. Inst.*, vol. 35, no. 1, pp. 101–115, 2015.

[9] G. T. Kalghatgi, “Auto-Ignition Quality of Practical Fuels and Implications for Fuel Requirements of Future SI and HCCI Engines,” *Sae*, no. 1, p. 239, 2005.

[10] G. Kalghatgi, H. Babiker, and J. Badra, “A Simple Method to Predict Knock Using Toluene, N-Heptane and Iso-Octane Blends (TPRF) as Gasoline Surrogates,” *SAE Int. J. Engines*, vol. 8, no. 2, pp. 2015-01–0757, 2015.

[11] Z. Liu, H., Yao, M., Zhang, B., Zheng, “Influence of Fuel and Operating Conditions on Combustion Characteristics of a Homogenous Charge Compression Ignition Engine,” *Energy & Fuels*, no. 23, pp. 1422–1430, 2009.

[12] J. P. Szybist and D. A. Splitter, “Pressure and temperature effects on fuels with varying octane sensitivity at high load in SI engines,” *Combust. Flame*, vol. 177, pp. 49–66, 2017.

[13] V. H. Rapp, W. J. Cannella, J. Chen, and R. W. Dibble, “Combustion Science and Technology Predicting Fuel Performance for Future HCCI Engines,” no. April 2015, pp. 37–41.

[14] I. Truedsson, W. Cannella, B. Johansson, and M. Tuner, “Development of New Test Method for Evaluating HCCI Fuel Performance,” *SAE Tech. Pap. Ser. 2014-01-2667*, 2014.

[15] D. Bradley and R. A. Head, “Engine autoignition: The relationship between octane numbers and autoignition delay times,” *Combust. Flame*, vol. 147, no. 3, pp. 171–184, 2006.

[16] J. A. Badra, N. Bokhumseen, N. Mulla, S. M. Sarathy, A. Farooq, G. Kalghatgi, and P. Gaillard, “A methodology to relate octane numbers of binary and ternary n-heptane , iso-octane and toluene mixtures with simulated ignition delay times,” *Fuel*, vol. 160, pp. 458–469, 2015.

[17] C. Pera and V. Knop, “Methodology to define gasoline surrogates dedicated to auto-ignition in engines,” *Fuel*, vol. 96, pp. 59–69, 2012.

[18] M. Christensen, A. Hultqvist, and B. Johansson, “Demonstrating the Multi Fuel Capability of a Homogeneous Charge Compression Ignition Engine with Variable Compression Ratio,” *SAE Tech. Pap.*, no. 724, pp. 1999-01–3679, 1999.

[19] S. Tanaka, F. Ayala, J. C. Keck, and J. B. Heywood, “Two-stage ignition in HCCI combustion and HCCI control by fuels and additives,” *Combust. Flame*, vol. 132, no. 1–2, pp. 219–239, 2003.

[20] M. Sjöberg and J. E. Dec, “Combined Effects of Fuel-Type and Engine Speed on Intake Temperature Requirements and Completeness of Bulk-Gas Reactions for HCCI Combustion Reprinted From : Homogeneous Charge Compression Ignition Engines 2003,” *Sae Tech. Pap. Ser.*, vol. 1, no. 3173, 2003.

[21] I. Truedsson, M. Tuner, B. Johansson, and W. Cannella, “Pressure Sensitivity of HCCI Auto-Ignition Temperature for Primary Reference Fuels,” *SAE Int. J. Engines*, vol. 5, no. 3, pp. 2012-01–1128, 2012.

[22] I. Truedsson, M. Tuner, B. Johansson, and W. Cannella, “Pressure Sensitivity of HCCI Auto-Ignition Temperature for Gasoline Surrogate Fuels,” *SAE Int. J. Engines*, vol. 5, no. 3, pp. 2012-01–1128, 2013.

[23] F. Contino, P. Dagaut, F. Halter, J.-B. Masurier, G. Dayma, C. Mounaim-Rousselle, and F. Foucher, “Screening method for fuels in homogeneous charge compression ignition engines: application to valeric biofuels,” *Energy & Fuels*, p. acs.energyfuels.6b02300, 2016.

[24] D. Splitter, B. Kaul, J. Szybist, and G. Jatana, “Engine Operating Conditions and Fuel Properties on Pre-Spark Heat Release and SPI Promotion in SI Engines,” *SAE Int. J. Engines*, vol. 10, no. 3, pp. 2017-01–0688, 2017.

[25] J. A. Gatowski, E. N. Balies, K. M. Chun, F. E. Nelson, J. A. Ekchian, and J. B. Heywood, “Heat Release Analysis of Engine Pressure Data,” *SAE Tech. Pap.*, 1984.

[26] T. Aroonsrisopon, D. Foster, T. Morikawa, and M. Lida, “Comparison of HCCI Operating Ranges for Combinations of Intake Temperature , Engine Speed and Fuel Composition,” *SAE Tech. Pap.*, no. 2002-01–1924, 2002.

[27] N. Atef, G. Kukkadapu, S. Y. Mohamed, M. Al Rashidi, C. Banyon, M. Mehl, K. A. Heufer, E. F. Nasir, A. Alfazazi, A. K. Das, C. K. Westbrook, W. J. Pitz, T. Lu, A. Farooq, C. J. Sung, H. J. Curran, and S. M. Sarathy, “A comprehensive iso-octane combustion model with improved thermochemistry and chemical kinetics,” *Combust. Flame*, vol. 178, pp. 111–134, 2017.

## Contact Information

Corresponding author, email:

Jean-Baptiste Masurier, jeanbaptiste.masurier@kaust.edu.sa

## Definitions/Abbreviations

| | |
|---|---|
| **HCCI** | Homogeneous Charge Compression Ignition |
| **RON** | Research Octane Number |
| **MON** | Motor Octane Number |
| **CFR** | Cooperative Fuel Research |
| **TDC** | Top Dead Center |
| **CA50** | Crank angle where 50% of the fuel has burnt |
| **CA** | Crank Angle |